ASIAN JOURNAL OF CIVIL ENGINEERING (BUILDING AND HOUSING) VOL. 8, NO. 2 (2007)
PAGES 183-201

NON-LINEAR SEISMIC SOIL-STRUCTURE INTERACTION ANALYSIS OF STRUCTURES BASED ON THE SUBSTRUCTURE METHOD

A. Gouasmia* and K. Djeghaba
Département de génie civil, Université Badji Mokhtar, BP 12 Annaba, 23000, Algérie

ABSTRACT

In this paper, a numerical model for wave induced vibrations in buildings is developed based on a substructure method by using original Matlab software developed by the authors. A dynamic analysis of the structure subjected to an incident wave field, is performed using the subdomain formulation. The structure is analysed with a finite element method and the unbounded soil domain is computed with a boundary element method using the Green's functions of a layered halfspace.

The problem of eigenfrequencies for embedded foundations in the frequency range of interest for seismic wave induced vibrations is addressed. A weakly singular boundary integral equation in elastodynamics for heterogeneous domains is presented, which combines the boundary integral equations in terms of the displacement and its normal derivatives. Based on an extensive parametric study, general conclusions are drawn for practical range of dimensionless parameters.

Insight in the effect of soil-structure interaction and the determining factors for seismic wave induced vibrations is obtained from the results of parametric study. The influence of the type of foundation (rigid or flexible, surface or embedded, slab strip or box foundation) is specially emphasized.

Keywords: soil-structure interaction, finite element method, boundary element method, Green's function, substructure method, MATLAB

1. INTRODUCTION

Vibrations in structures, especially in buildings may cause the following problems. Depending on the amplitudes of structural vibrations, the resulting may range from nuisance to occupants to life threat and full damage to buildings.

Following the new concept in structural design based on the so-called Performance Based Design (PBD), damage caused to buildings is described as a change in the properties and/or position of structural members. Among the possible consequences, we may distinguish,

* Email-address of the corresponding author: gouasmia_abdelhacine@yahoo.fr

failure of beams and/or columns, reduction of the structural capacity of a member or the whole structure and loss of serviceability due to cracks.

The increasing interest for the problem of soil structure interaction effects (SSI) for ordinary structures, which are the most vulnerable among the built in environment has triggered off the need for a better insight in the physical phenomena involved in SSI problems. Therefore, the development of a numerical prediction model that takes into account SSI effects is treated in this paper.

In almost all seismic building codes, the structure response and foundation loads are computed neglecting the soil-structure interaction. However there is evidence that some structures founded on soft soils are vulnerable to SSI. Examples are given by Gazetas and Mylonakis in 1998 [1].

This has been recognized in some codes as Eurocode 8, where it is stated clearly that "The effects of dynamic soil-structure interaction shall be taken into account in the case of:

- structures where P-δ effects play a significant role;
- structures with massive or deep seated foundations;
- slender tall structures;
- structures supported on very soft soils, with average shear wave velocity less than 100 m/s.

The effects of soil-structure interaction on piles shall be assessed..."

In dealing with the analysis of dynamic soil-structure interaction, one of the most difficult tasks is the modeling of the unbounded nature of soil media. Many numerical methods have been developed to solve this kind of problem, such as transmitting boundaries of different kinds, boundary elements, and infinite elements and their coupling procedures.

There are two main approaches for analyzing soil-structure interaction, namely the direct method and the substructure method. These methods are well documented in two textbooks by Wolf in 1985 [2]. Both methods are still being developed to achieve the desired results.

The response of the structure due to the incident wave field is calculated using a subdomain formulation for dynamic SSI [3]. The structure having a finite dimension is analyzed using a numerical approach as the FEM. The semi-infinite soil medium is treated by means of the BEM, using the Green's functions for the homogeneous or the layered half-space, which automatically takes into account the radiation condition. This coupled method FEM/BEM will result in an important reduction in the number of degrees of freedom.

Only the interface between the structure and the soil needs to be discretised, reducing the spatial dimensions of the problem by one and making three-dimensional (3D) calculations feasible.

This kind of problem (SSI) belongs to the field of earthquake engineering, where the response of the structure is calculated due to an incident wave field where the frequency content of typical earthquakes is in between the range 0-10Hz.

The use of a full Finite Element (FE) model for a single building is advocated to assess vibration problems. In practice, it used to be that FE modeling and dynamic SSI analysis is only performed for buildings of considerable societal importance (nuclear power plants, hospitals) and for critical work spaces as micro-electronics laboratories and rarely for ordinary buildings, that is residential buildings.

This particular problem is considered, and this case was well documented within the

frame of experimental studies through PEER and NEES reports. Furthermore, building a complete structural model allows to obtain a better insight in the decay of vibrations from the far field (free field) to the near field and the soil foundation (this is part of the soil adjacent to the foundation where most of the nonlinearities will happen), as well as the amplification per story over the height of the building. This would not have been possible with a simple 1D model of the structure on a half-space.

The original contributions of this research work are the following:

A clear overview of the numerical modeling for wave induced vibrations in buildings is given. For this purpose, a validated model coupling soil to structure is used. Plane incident waves are assumed in the modeling of SSI due to earthquakes as the distance between the epicenter and the region of interest is usually very large.

A parametric study to determine factors influencing wave propagation induced vibrations in buildings is undertaken. The conclusions are based on a limited number of well chosen experimental test cases. The influence of the type of foundation on the overall structural response is thoroughly investigated. The availability of test results of a seven-storey reinforced concrete hotel building located in the city of Van Nuys in Los Angeles [4] enabled us to perform a large number of case studies, such as the effect of SSI in vibration isolation.

2. SOIL STRUCTURE INTERACTION PROBLEM FORMULATION

Foundation wave induced vibrations are caused by earthquakes that pass through the soil (Figure 1). A dynamic excitation is generated due to the interaction between the foundations and the soil, which requires the solution of a dynamic soil-structure interaction problem at the interface $\sum$ between the foundation and the soil. Waves generated in the far field in the soil domain Ω_s^{ext} and impinge on the foundation of the structure Ω_b, which leads to a DSSI problem at the interface $\sum$ between the soil and the structure.

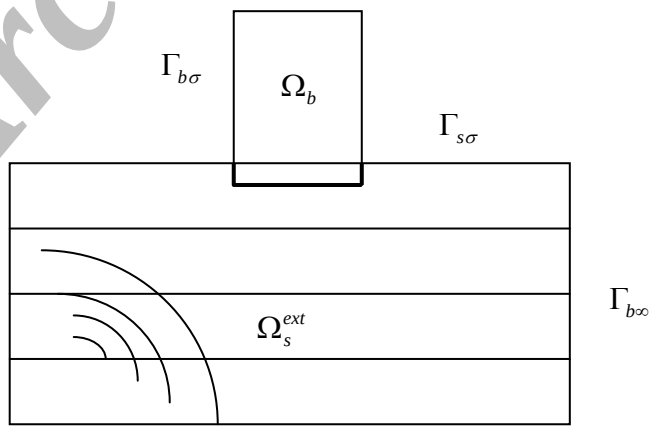

Figure 1. Geometry and notations of the subdomains

The incident wave field interacts with the structure and generates vibrations. The foundation and the structure are coupled through the soil. It is assumed, however, that the presence of the structure hardly affects the impedance of the soil below the foundation, when the width of the structure (footprint dimension) is much larger than the dominant wavelength in the soil. Therefore, it is assumed in this research that the DSSI problem at the soil and the structure can be uncoupled. This is a wide-spread assumption in the field of earthquake engineering. Due to this uncoupling, a solution procedure in two stages can be applied.

First, the soil model is used to predict the incident wave field u_{inc} due to the passage of waves, accounting for dynamic foundation-soil interaction (Figure 1). The incident wave field u_{inc} is defined on the semi-infinite layered soil domain $\Omega_s = \Omega_s^{ext} \cup \Omega_s^{int}$ without excavation of the interior soil domain Ω_s^{int}. Dynamic foundation-soil interaction is accounted for by means of the subdomain formulation proposed by Aubry et al.[3]. The continuity of displacements is accounted for along the foundation-soil interface $\sum_{rs}$. An analytical beam model is used for the foundation, while the soil is modeled using boundary elements.

The next step is the application of the incident wave field to the structure Ω_b and the response is computed, accounting for dynamic soil-structure interaction (DSSI).

The subdomain formulation proposed by Aubry et al.[3] has been implemented in a MATLAB computer program, which has been developed to solve dynamic soil structure problems.

3. GOVERNING EQUATIONS OF MOTIONS FOR THE DISPLACEMENT IN THE STRUCTURE

First, the structure Ω_b is considered (Figure 1). The boundary $\Gamma_b = \Gamma_{b\sigma} \cup \sum$ of the structure Ω_b is decomposed into a boundary $\Gamma_{b\sigma}$ where tractions $\bar{t}_b$ are imposed and the soil-structure interface $\sum$. The displacement vector u_b of the structure satisfies the following Navier equation and boundary conditions:

$$\mathrm{div}\sigma_b(u_b) + \rho_b b = -\rho_b \omega^2 u_b \quad \text{in} \quad \Omega_b \tag{1}$$

$$t_b(u_b) = \bar{t}_b \quad \text{on} \quad \Gamma_{b\sigma} \tag{2}$$

$$u_b = u_s \quad \text{on} \quad \sum \tag{3}$$

$$t_b(u_b) + t_s(u_s) = 0 \quad \text{on} \sum \tag{4}$$

where $\rho_b b$ is the body force on the structure and t (u)= σ(u) •n the traction vector on a boundary with a unit outward normal vector n.

4. FORMULATION OF THE EQUATIONS FOR THE DISPLACEMENTS IN THE SOIL

The displacement vector u_s of the soil satisfies Navier equation and the following boundary conditions:

$$\mathrm{div}\sigma_s(u_s)+\rho_s b=-\rho_s\omega^2 u_s \quad \text{in} \quad \Omega_s^{ext} \tag{5}$$

$$t_s(u_s)=0 \quad \text{on} \quad \Gamma_{s\sigma} \tag{6}$$

$$u_s=u_b \quad \text{on} \quad \sum \tag{7}$$

$$t_b(u_b)+t_s(u_s)=0 \quad \text{on} \quad \sum \tag{8}$$

where it is assumed in equation (5) that the body force $\rho_b b$ represents a constant that is directly applied on the semi-finite layered half-space Ω_s^{ext} and causes an incident wave field in the soil (Figure 1).

The displacement vector u_s in the soil is generally decoupled using a Helmholtz decomposition, which results in a set of uncoupled partial differential equations representing the longitudinal and shear wave propagation.

5. VARIATIONAL FORMULATION

In this section, the equation of motion of the DSSI problem is approached by a variational form [5]. The principle of virtual work states that the equilibrium of the structure requires that for any virtual displacement field δv imposed on the structure, the sum of the virtual work of the internal and the inertial forces is equal to the total virtual work of the external loads, which results in the following weak form integral equation:

$$\begin{aligned}&\int_{\Omega_b}\varepsilon(\delta v):\sigma_b(u_b)d\Omega-\omega^2\int_{\Omega_b}\delta v.\rho_b u_b d\Omega\\&=\int_{\Omega_b}\delta v.\rho_b b d\Omega+\int_{\Omega_b}\delta v.\bar{t}_b d\Gamma+\int_{\Omega_b}\delta v.t_b(u_b)d\Sigma\end{aligned} \tag{9}$$

The volume integrals over Ω_b will result in the mass and the stiffness matrix of the structure. As the structure Ω_b has a finite dimension, the mass and the stiffness matrix can be calculated using the FEM. As is well known FEM procedures are widely used in structural analysis, only the basic principles of the FEM, needed in the discretisation of the scalar equation (9), will be presented. Over the boundary $\sum$, the tractions $\mathbf{t}_s(\mathbf{u}_{sc}(\mathbf{u}_b))$ and $\mathbf{t}_s(\mathbf{u}_{inc}+\mathbf{u}_{d0})$ given in the surface integral are computed using the BEM.

For any virtual displacement field $\delta \underline{v}$ the virtual work equation must hold, and then the equation (9) is equivalent to:

$$(K_b - \omega^2 M_b + K_s)\underline{u}_b = f_b \tag{10}$$

The stiffness matrix $\mathbf{K}_b$ and the mass matrix $\mathbf{M}_b$ of the structure are given by:

$$K_b = \int_{\Omega_b} B_b^T D B_b d\Omega \tag{11}$$

$$M_b = \int_{\Omega_b} N_b^T \rho_b N_b d\Omega \tag{12}$$

FEM is used to calculate the stiffness matrix $\mathbf{K}_b$ and the mass matrix $\mathbf{M}_b$ of the structure. The dynamic stiffness matrix $\mathbf{K}_s$ of the semi-finite layered half-space is given by:

$$K_s = \int_{\Sigma} N_b^T t_s(u_{sc}(N_b)) d\Sigma \tag{13}$$

The vector $\mathbf{f}_b$ due to the external forces on the structure is defined by:

$$f_b = \int_{\Omega_b} N_b^T \rho_b b d\Omega + \int_{\Gamma_{b\sigma}} N_b^T \bar{t}_b d\Gamma - \int_{\Sigma} N_b^T t_s(u_{inc} + u_{d0}) d\Sigma \tag{14}$$

A boundary element approach is used for the calculation of the tractions $\mathbf{t}_s(\mathbf{u}_{sc}(\mathbf{N}_b))$ in the dynamic stiffness matrix $\mathbf{K}_s$ of the soil and $\mathbf{t}_s(\mathbf{u}_{inc}+\mathbf{u}_{d0})$ in the external force vector $\mathbf{f}_b$. For the case of a horizontally layered half-space, if the BEM is based on the Green's functions, only a discretisation of the interface $\sum$ between the soil and the structure is required and the number of unknowns is considerably reduced [6].

The solution of the elastodynamics problem on the exterior domain Ω_s^{ext} having an embedded region Ω_s^{int} of finite extent, using a discretisation form of a displacement boundary integral equation, is not unique at the eigenfrequencies of the embedded interior domain Ω_s^{int} with Dirichlet boundary conditions along the soil-structure interface $\sum$ and free boundary conditions along the free surface Γ_{s0} [7,8,9]. This numerical deficiency problem occurs in the high frequency range, and it depends on the geometry of the foundation and the stiffness of the excavated soil. Therefore, the problem of fictitious frequencies is not very stringent for applications in seismic engineering, where the excitation frequencies are low (typically between 0 and 10 Hz).

In the frequency domain hysteretic damping can be introduced using the correspondence principle and by replacing the stiffness matrix $\mathbf{K}_b$ by a complex stiffness matrix $K_b(1+2\xi i)$ with ξ a damping ratio. The introduction of hysteretic damping in the equilibrium equation (10) results in:

$$(\mathrm{K}_b(1+2\xi i)-\omega^2\mathrm{M}_b+\mathrm{K}_s)\underline{\mathrm{u}}_b=\mathrm{f}_b \tag{15}$$

If viscous damping is introduced, the equilibrium equation (10) of the SSI problem becomes:

$$(\mathrm{K}_b+i\omega\mathrm{C}_b-\omega^2\mathrm{M}_b+\mathrm{K}_s)\underline{\mathrm{u}}_b=\mathrm{f}_b \tag{16}$$

In the present work, proportional damping corresponding to defining a damping ratio $\xi_m(m=1,...,q)$ for each mode ψ_m of the structure is used. The advantage of using proportional damping will result in a decoupled equilibrium equation. The corresponding damping matrix C_b is then computed as follows:

$$\mathrm{C}_b=\mathrm{M}_b\underline{\Psi}\mathrm{diag}(2\xi_m\omega_m)\underline{\Psi}^{\mathrm{T}}\mathrm{M}_b \tag{17}$$

where the vector $\underline{\Psi}$ represents the eigenmodes $\underline{\psi}_m$ at the corresponding eigenfrequencies ω_m of the structure. In this thesis, the same damping ratio is used for all modes.

Rayleigh damping is defined as a special case of proportional damping where the damping matrix C_b is equal to:

$$\mathrm{C}_b=\alpha\mathrm{M}_b+\beta\mathrm{K}_b \tag{18}$$

Where the parameters α and β can be calculated by $\alpha=2\xi\omega_m\omega_n/(\omega_m+\omega_n)$ and $\beta=2\xi/(\omega_m+\omega_n)$, with ω_m and ω_n being two specific eigenfrequencies and ξ the damping ratio that applies to both frequencies.

6. NUMERICAL APPLICATION

The proposed analysis model is applied to study the dynamic responses of structures to earthquake excitation in the time domain. The computational model employed in this section is shown in Figure 2. The parameters of the model are given in Figure 4. The accelerogram (E-W component) for the Erzincan earthquake of 1992 (Figure 3) is employed as the horizontal ground motion applied to the analysis model.

Three different foundations are considered for the parametric building. Figure 2 shows the geometry of a structure with a concrete slab foundation, an embedded concrete strip foundation and an embedded concrete box foundation. The foundation has a length Lx = 12m and a width Ly = 6m. The thickness of the slab foundation is equal to 0.3 m. The bottom slab of the embedded box foundation has a thickness of 0.3 m. The thickness of the foundation walls is also equal to 0.3 m. The embedment of the box foundation is equal to 2 m. The width of the strips is equal to 1.0 m and the embedment equals 1.0 m.

The following material properties for concrete are used: a Young's modulus E = 33300 x10^6 N/m^2, a Poisson's ratio ν = 1/3 and a density ρ = 2500 kg/m^3

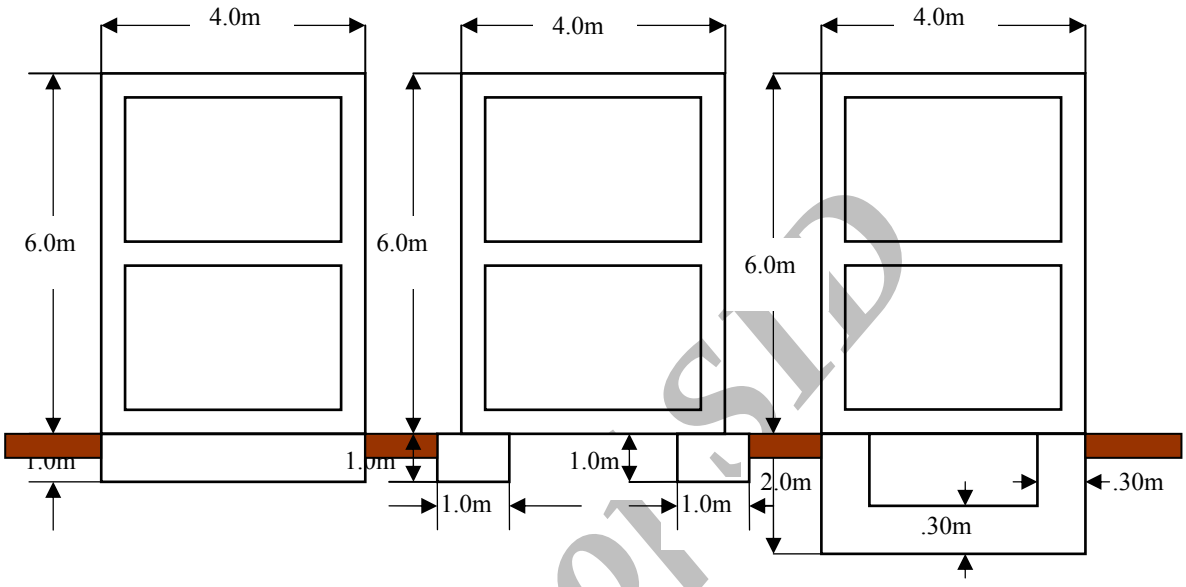

a. Slab foundation. b. Strip foundation. c. Box foundation.

Figure 2. Geometry of the (a) slab, (b) strip and (c) box foundation.

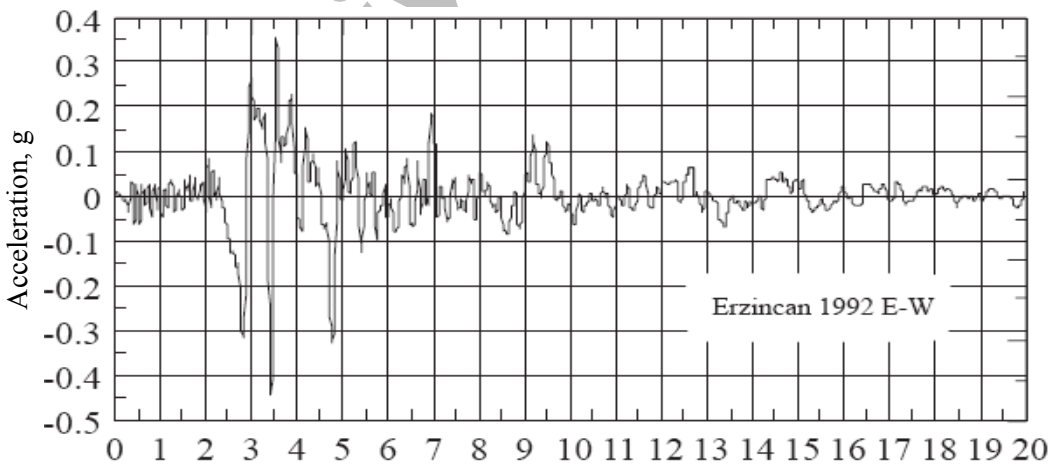

Figure 3. Erzincan acceleration time history at the ground surface (max. 0.44g)

7. IMPORTANCE OF SSI FOR DIFFERENT FOUNDATION TYPES

7.1 Results in different points in the structure

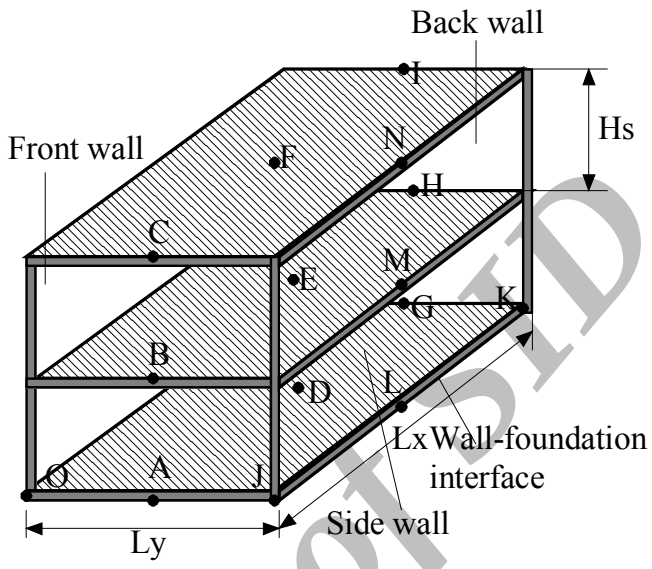

Figure 4. Building characteristics and point location for parametric calculation

In the following, the results are obtained for two cases: considering SSI and neglecting SSI which will be referred to as the no-SSI.

The effect of SSI on the amplitude of the structural response is twofold. The peak response, which occurs at the eigenfrequency of the dynamic system, shifts to lower frequencies due to a decrease in the stiffness of the soil, while the geometrical damping (called also radiation damping) in the unbounded soil generally causes a decrease in amplitude.

In the no-SSI case, the soil is assumed to be rigid with respect to the structure, the foundation will follow the incident wave field and no SSI occurs. The behaviour of a structure subjected to an incident wave field depends on the difference in stiffness between the structure and the soil.

In this no-SSI case, the response is calculated for two situations. The calculation of the response using all foundation modes is termed no-SSI-FF (FF:Flexible Foundation), when the response is estimated using only the rigid body modes of the foundation, this is called no-SSI-RF (RF:Rigid Foundation).

The difference in the SSI, the no-SSI-RF and the no-SSI-FF calculation is first investigated using the vertical displacement at foundation level for the three foundation types.

Figure 5 shows the results of the three calculations for the SSI, the no-SSI-FF and the no-SSI-RF calculation for the slab foundation. The incident wave front, which is indicated also

in Figure 5, is approximated properly by the 20 linear combination modes of the foundation with free boundary conditions in the no-SSI-FF calculation. for the building resting on a soft soil, no deformation of the walls occurs and the overall deformation of the building is dominated by rigid body motion. In the case of a structure resting on a stiff soil, the walls deform following the ground motion. In addition, the presence of a stiff foundation prohibits the walls to deform.

The no-SSI-FF calculation case gives rise to non physical deformation of the walls and unsatisfactory results.

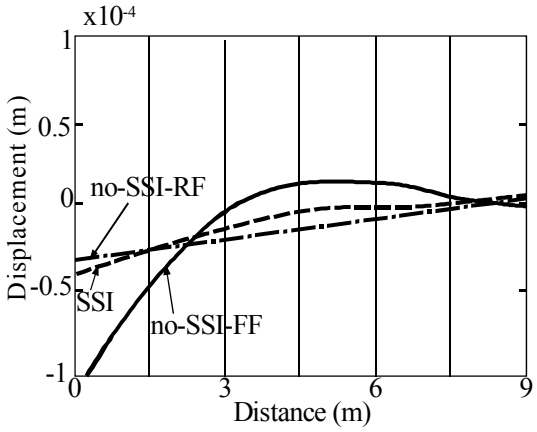

Figure 5. Vertical displacement of the foundation-structure interface JK at t=-0.35s. for the box foundation

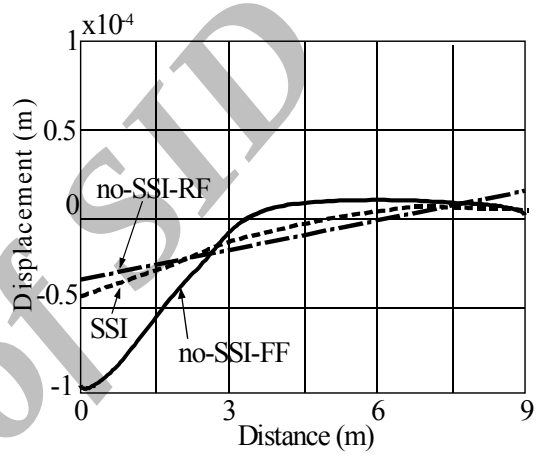

Figure 6. Vertical displacement of the foundation-structure interface JK at t=-0.33s. for the box foundation

A no-SSI-RF case is a solution to this kind of problems, as the rigid body motion of the foundation do not deform the walls. The resulting displacements of the wall-foundation interface better approximate the displacements of an SSI case than the no-SSI case when using all foundation modes. A no-SSI-FF case results in a foundation displacement that is very close to the incident wave field.

Figure 6 shows the results of the SSI, the no-SSI-FF and the no-SSI-RF case for the strip foundation. The incident wave field is well approximated by the 20 linear foundation modes with free boundary conditions in the no-SSI-FF case.

Figure 7 shows the results of the SSI, the no-SSI-FF and the no-SSI-RF case for the box foundation. It is shown from this figure, that this number of foundation modes is not sufficient to approximate the incident wave field at the foundation interface by means of the least squares approximation, because the box type foundation mode shapes are dominated by bending modes of the bottom slab. Especially for the box foundation, the SSI case results in a linear vertical displacement of the wall-foundation interface.

Figure 8 and 9 show the time history of the horizontal velocity in the points A and C for the SSI, the no-SSI-FF and the no-SSI-RF cases (Figure 4.5). As expected, the horizontal response in point A is larger for the box foundation type due to the rocking motion

component that arises for an embedded foundation. This effect is less important for the strip foundation type as the embedment is generally small. Bending effects around the y-axis increase the response in the horizontal direction in point C in comparison with point A.

Figure 10, 11 and 12 show the time history of the vertical velocity of points A, C and G. The response in the vertical direction is almost the same for points A and C due to the high structural stiffness in that direction. In point A, the incident wave field is little affected by the presence of the building, while the response in point G is affected by the rigid body motion of the walls, since the wave front field is affected by the presence of the building as it travels from point A to point G. In the low frequency range, the no-SSI-RF case is a very good approximation for the response of the building in a calculation using SSI.

Figure 13 shows the time history of the vertical response for both, slab and box foundation types in point D. Due to the relative flexibility between the slab foundation and the soil, the response of the centre of the foundation is very close to the incident wave field. It is also noted, that the assumption of a rigid foundation yields an underestimation of the response of the foundation. The box foundation is more rigid, and follows the global rigid body motion of the whole building. Therefore, the SSI effects are more important in the latter case.

The problem of excessive vibrations is very often related to the slab. Figure 14, 15 and 16 show the time history of the vertical velocity in points B, M and H along the boundary of the slab (Figure 4.5). As there is a difference between the results in the slab edge points, a plate model of this slab excited by a non-uniform input motion is required. In current design practice, simple rules expressing the decay of vibrations from the free field to the basement, as well as the amplification over the height of the building, are used in order to investigate vibration problems on the slab.

Figure 17 shows the time history of the vertical response in point E in the centre of the first floor. The frequency content is dominated by a peak at 70.72 rad/sec, corresponding to the first mode of vibration of the structure clamped at its base. The difference between the SSI and no-SSI cases is explained as follows.

The incident wave front field adds energy to the structure through the soil-structure interface. In a calculation without SSI effects, the structure is referred to as a closed system after the incident wave field has passed, and all the energy is dissipated through material damping in the structure.

In contrast to this, the energy will be dissipated through radiation damping in the soil in a SSI case. The response on the floors is dominated by the local floor modes, resulting in a resonance. Due to the presence of radiation damping, the effect of SSI results in an increased attenuation of the floor response (Figure 17). In contrast to the slab, the difference between the SSI and the no-SSI calculation is smaller for the walls.

It is generally admitted that the SSI effects increases when the soil is more flexible and the structure is stiffer. The building considered in this study has a stiff superstructure, which predominantly acts as a rigid body. The same conclusions hold for the strip foundation and for the box foundation types. Therefore, a good approximation of the structural behaviour in stiff points is therefore obtained using a no-SSI-RF calculation case. However, in points located on the slab foundation (point D) or on other points (E and F) resonance of the floors is attenuated quickly due to radiation damping and SSI calculation is therefore recommended.

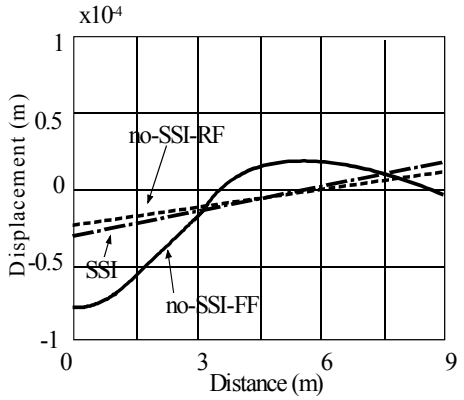

Figure 7. Vertical displacement of the foundation-structure interface JK at t=-0.31s. for the box foundation

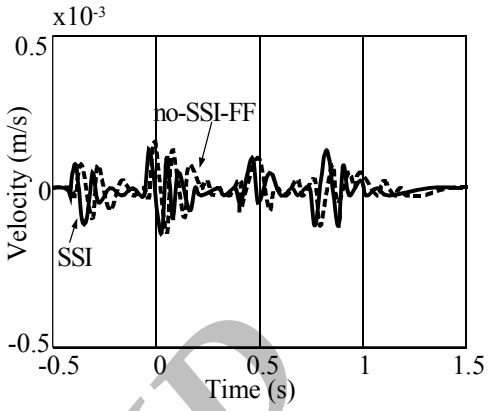

Figure 8a. Time history of the horizontal response in point A (front wall-foundation edge) for the slab foundation

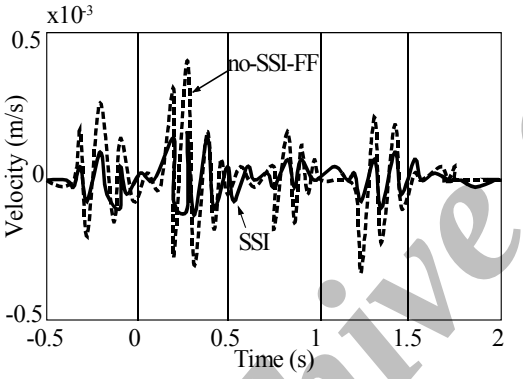

Figure 8b. Time history of the horizontal response in point A (front wall-foundation edge) for the slab foundation

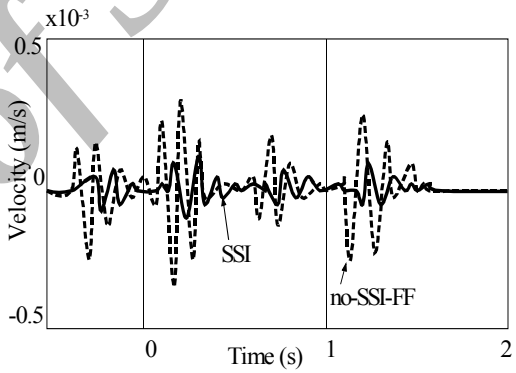

Figure 8c. Time history of the horizontal response in point A (front wall-foundation edge) for the box foundation

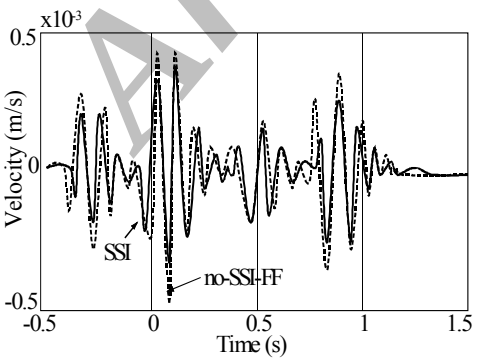

Figure 9a. Time history of the horizontal response in point C, for the slab foundation

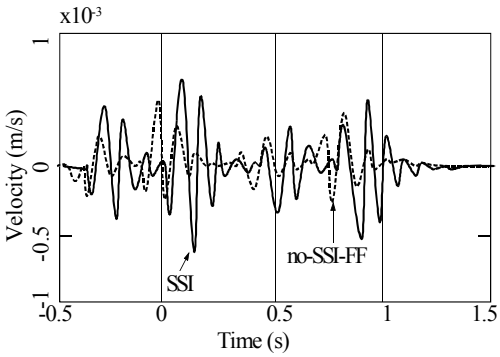

Figure 9b. Time history of the horizontal response in point C, for the strip foundation

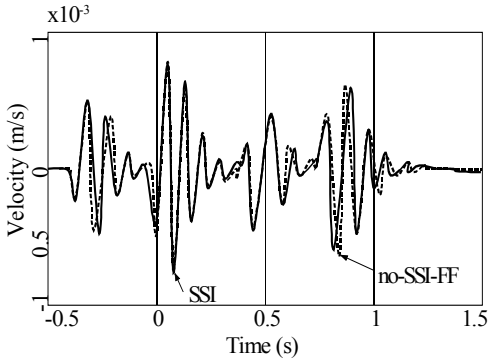

Figure 9c. Time history of the horizontal response in point C, for the box foundation

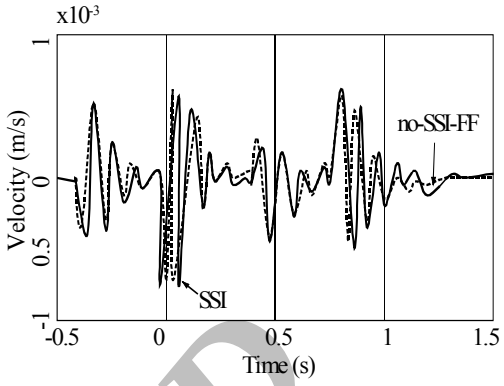

Figure 10a. Time history of the horizontal response in point C, for the slab foundation

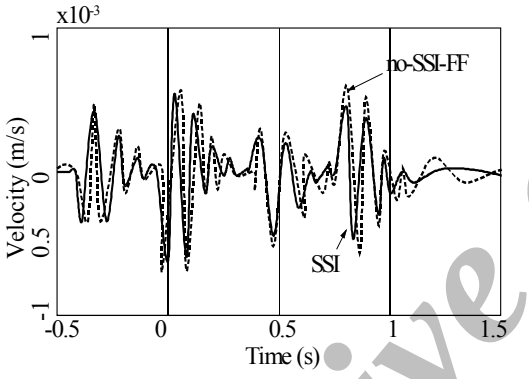

Figure 10b. Time history of the vertical response in point A, for the strip foundation

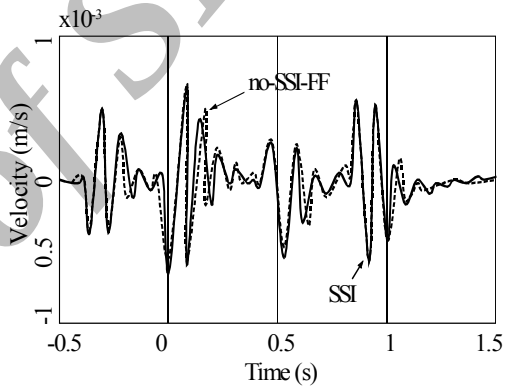

Figure 10c. Time history of the vertical response in point A, for the box foundation

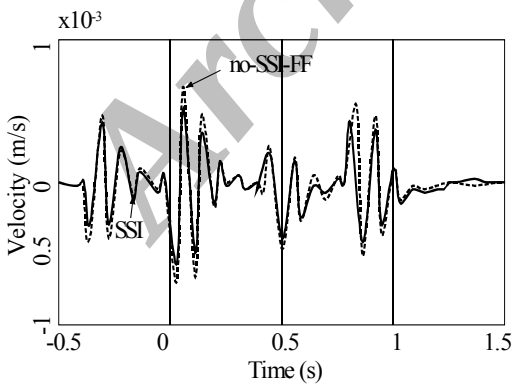

Figure 11a. Time history of the vertical response in point C, for the slab foundation

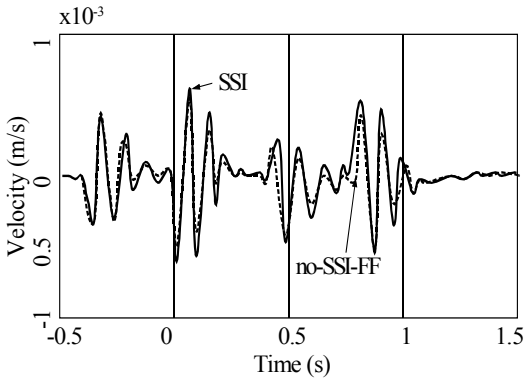

Figure 11b. Time history of the vertical response in point C, for the strip foundation

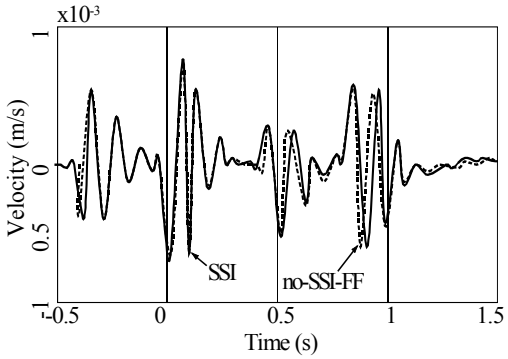

Figure 11c. Time history of the vertical response in point C, for the box foundation

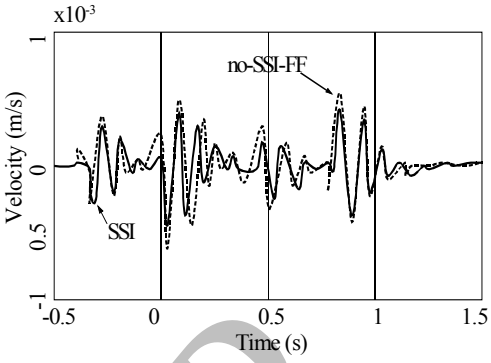

Figure 12a. Time history of the vertical response in point G, for the slab foundation

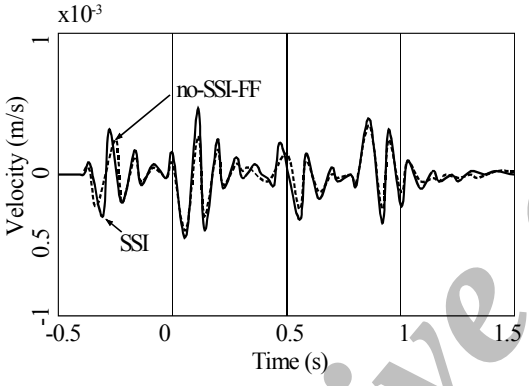

Figure 12b. Time history of the vertical response in point G, for the strip foundation

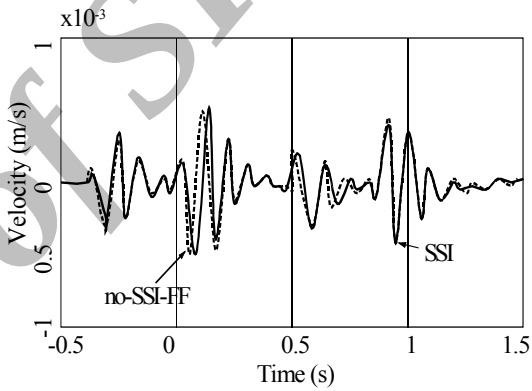

Figure 12c. Time history of the vertical response in point G, for the box foundation

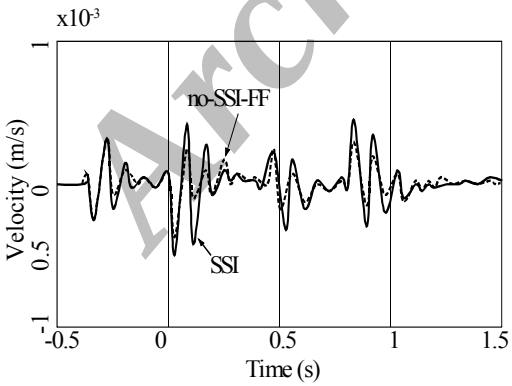

Figure 13a. Time history of the vertical response in point D, for the slab foundation

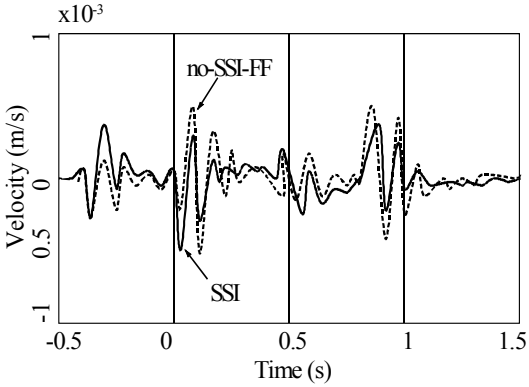

Figure 13b. Time history of the vertical response in point D, for the box foundation

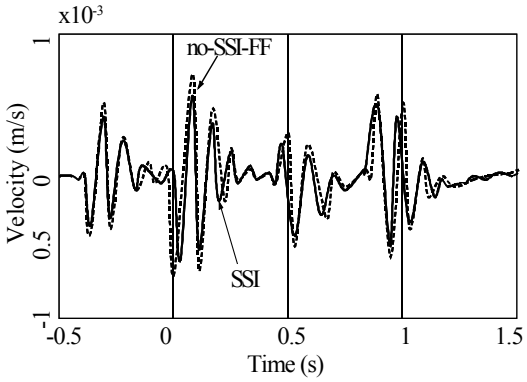

Figure 14a. Time history of the vertical response in point B, for the slab foundation

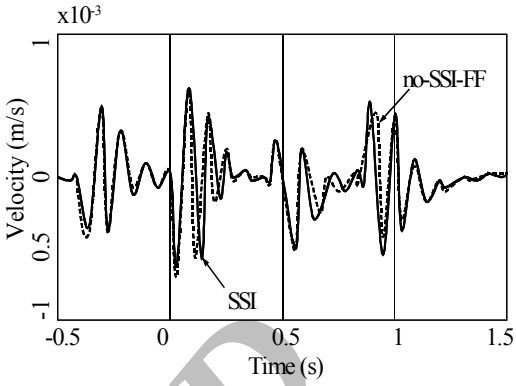

Figure 14b. Time history of the vertical response in point B, for the strip foundation

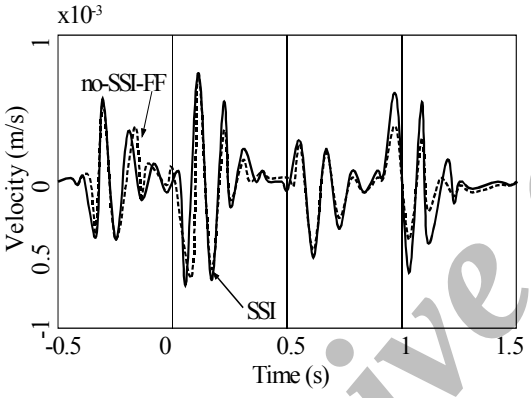

Figure 14c. Time history of the vertical reponse in point B, for the box faundation

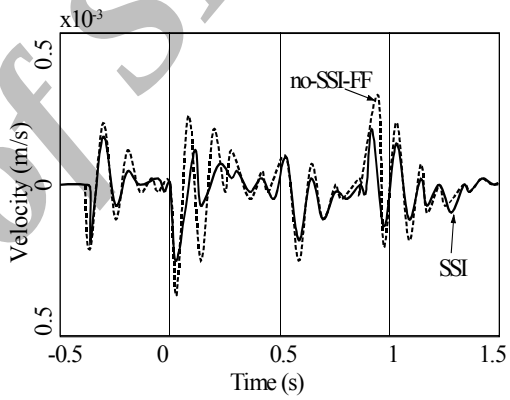

Figure 15a. Time history of the vertical reponse in point M, for the slab foundation

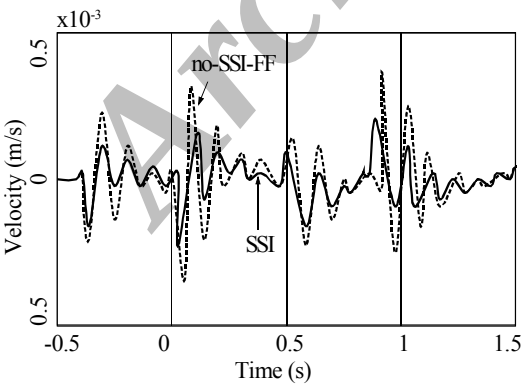

Figure 15b. Time history of the vertical reponse in point M, for the strip foundation

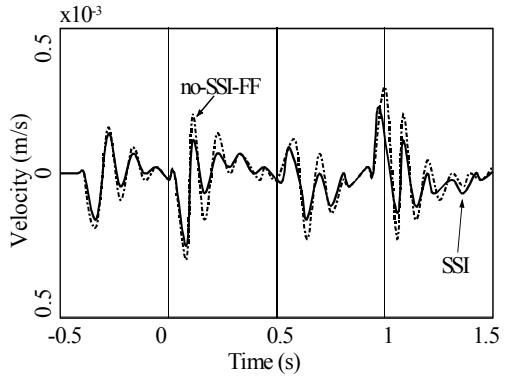

Figure 15c. Time history of the vertical reponse in point M, for the box foundation

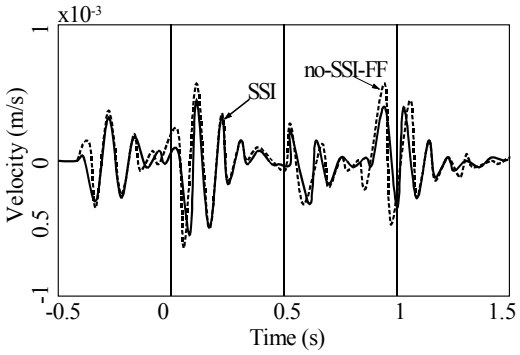

Figure 16a. Time history of the vertical reponse in point H, for the slab foundation

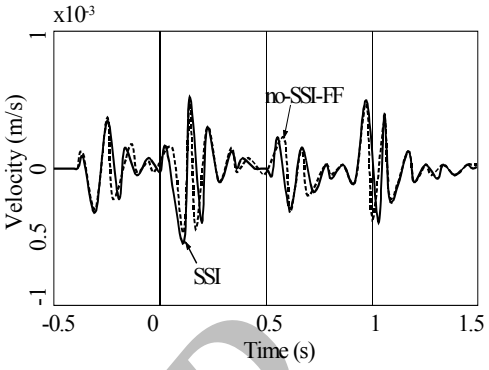

Figure 16b. Time history of the vertical reponse in point H, for the strip foundation

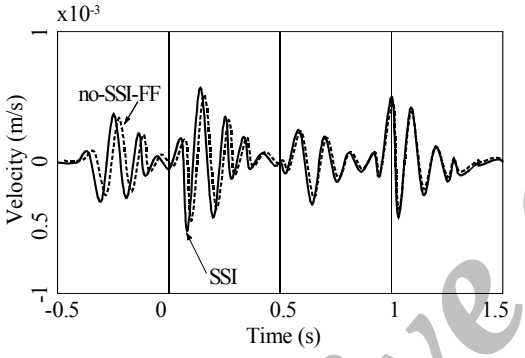

Figure 16c. Time history of the vertical reponse in point H, for the box foundation

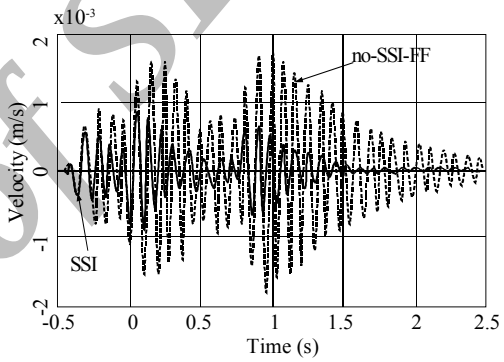

Figure 17a. Time history of the vertical reponse in point E, for the slab foundation

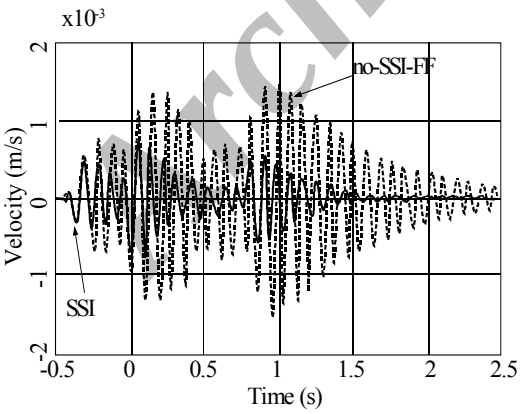

Figure 17b. Time history of the vertical reponse in point E, for the strip foundation

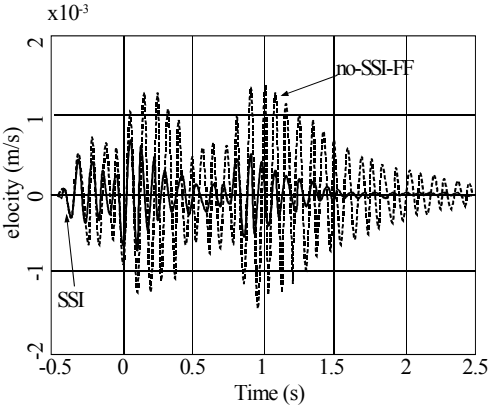

Figure 17c. Time history of the vertical reponse in point E, for the box foundation

8. CONCLUSIONS

A numerical model for the prediction of wave induced vibrations in buildings has been developed and used for large parametric analysis. The coupled soil-structure system takes account of the free field wave induced vibrations in buildings, both models are based on a subdomain formulation approach for dynamic SSI problems. This approach is not novel, in a sense that it has been applied before, to the seismic analysis of structures. However, a substantial contribution of this work is the application to wave induced vibrations, and measures are taken against the occurrence of fictitious eigenfrequencies.

First the numerical model for the prediction of vibrations in buildings due to wave front field is elaborated. A dynamic foundation-soil-structure interaction problem is solved to compute the incident wave field, which is subsequently applied to the structure. The response in the structure is calculated using a subdomain formulation. A FEM is applied for the structure, whereas the unbounded soil domain is computed with a BEM using the Green's functions of a homogeneous or layered half-space domain. The subdomain approach is programmed in a finite element MATLAB code, accounting for dynamic SSI.

A parametric study on the determining factors for wave induced vibrations in buildings has been performed, the response of the building has been calculated for a slab, a strip and a box foundation. The importance of SSI for the three foundation types in the dynamic SSI problem has been investigated. The stiffness of the soil has also been varied. The conclusions from the investigation of the modal characteristics of the structure and the response in different points in the structure are summarized as follows:

1. For the calculation of the response of the structure, a decomposition of the displacement vector of the structure into modes of the superstructure fixed (clamped) at the base and the quasi-static transmission of the free foundation modes into the superstructure is performed. Because of the walls' rigidity, the free foundation modes do not properly represent the kinematics of the foundation, which is prevented to deform along the joint between the foundation and the walls. Therefore, a high number of modes of the foundation (20) has been used, accounting for the additional 20 modes of the superstructure, the total number of modes is twice as high as the number of modes that would be used for the total structure including the foundation. The Craig-Bampton substructure method, that distinguishes between the modes of the foundation and the superstructure, is a valuable tool to a modal decomposition based on the modes of the total structure, as it does not require a new dynamic SSI calculation when the properties of the structure are changed.
2. Due to the effect of the wall's stiffness, no wall deformation modes appear in the frequency range of interest. In general, two possible sceneries may occur: (1) if the building is resting on a soft soil, no deformation of the walls occurs and the overall motion of the building is dominated by rigid body kinematics; (2) in the case of a structure resting on a stiff soil, the walls deformation follows the ground motion in a fully quasi-static way. This has major consequences for vibration inducing damage to buildings such as wall cracking, caused by excessive deformations, that is more likely to occur in the case where there is a quasi-static transmission of the ground motion into the walls.

3. The stiffness of the soil plays an important role in the free field response. Higher vibration amplifications occur in the case of a soft soil.
4. When dynamic SSI effects are neglected, the assumption that the motion of the foundation is equal to the incident wave motion results in unrealistic wall deformations when the structure is relatively rigid compared to the rigidity of the soil. Allowing only for a rigid body motion of the foundation, results in a better average of the wall displacements. When dynamic SSI effects are taken into account, the loss of energy due to radiation damping in the soft soil is beneficial. In general, peak amplitudes decrease and the frequency content shifts to lower frequencies. The importance of SSI analysis for structures founded on soft soil conditions is demonstrated by this example.
5. The response of the floors is dominated by local bending modes, dynamic SSI effects results in an increased attenuation of the floor response due to radiation damping in the soil.
6. When the slab foundation is flexible compared to the stiffness of the soil. The eigenfrequency of the first flexible eigenmode of the slab is in the frequency range of interest. Therefore, the response of the centre of the foundation is close to the incident wave field. The box foundation type is more rigid and follows the global rigid body kinematics of the entire building. Therefore, the dynamic SSI effects are more important in this case.
7. The height of the building seriously affects the horizontal response. Bending of the structure increases to a large extent the horizontal motion. The peak amplitude decreases and the frequency content shifts to lower frequencies. This example shows the importance of SSI effects on tall structures.
8. The results of the parametric study have shown that the influence of the foundation type is small. The highest vibration motions occur in the structure with a box foundation, although, the differences with the other types of foundations are not significant.

The results obtained from the parametric study allow for an effective estimate of vibration levels in new-built and existing structures and to develop efficient and cost-effective vibration isolation systems.

REFERENCES

1. Gazetas, G. and Mylonakis G., Seismic soil-structure interaction: new evidence and emerging issues. Geotechnical Earthquake Engineering and Soil Dynamics III ASCE, eds. Dakoulas, P., Yegian, M.K., and Holtz R. D., **2**(1998) 1119-1174.
2. Wolf, J.P., 1985. Dynamic soil-structure interaction. Prentice Hall.
3. Aubry, D., and Clouteau D., 1992. A subdomain approach to dynamic soil-structure interaction. In Davidovici, D. and Clough R.W., editors, 1992. Recent Advances in Earthquake Engineering and Structural Dynamics, pages 251-272. Ouest Editions/AFPS, Nantes.
4. Trifunac, M.D., and Hao T.Y., 2001. 7-Story reinforced concrete building in Van Nuys, California. Report CE 01-05, Dept. of civil Engineering University of Southern California, Los Angeles, California, U.S.A.

5. Hughes, T.J.R., The finite element method: linear static and dynamic finite element analysis. Prentice-Hall, Englewood Cliffs, New Jersey, 1987.
6. Apsel, R.J. and Luco J.E., On the Green's functions for a layered half-space. Part II. Bulletin of Seismological Society of America, **73**(1983) 931-951.
7. Burton, A.J. and Miller G.F., The application of integral equation methods to the numerical solution of some exterior boundary-value problems. In Proceedings of the Royal Society of London, **323**(1971) 201-210.
8. Chen, J.T., Chen, K.H. and Chen C.T., 2002. Adaptive boundary element method of time-harmonic exterior acoustics in two dimensions. Computer Methods in Applied Mechanics and Engineering, 191:3331-3345.
9. Rizzo, F.J., Shippy, D.J. and Rezayat M., 1985. A boundary integral equation method for radiation and scattering. International journal for numerical methods in engineering, 21:115-129.
10. MATLAB Partial Differential Equation Toolbox and User's Guide, 1996.